ChemComm

Understanding and Controlling the Metal-Directed Assembly of Terpyridine-Functionalized Coiled-Coil Peptides

Journal:	*ChemComm*
Manuscript ID	CC-COM-05-2019-003496.R1
Article Type:	Communication

COMMUNICATION

Understanding and Controlling the Metal-Directed Assembly of Terpyridine-Functionalized Coiled-Coil Peptides

Received 00th January 20xx,
Accepted 00th January 20xx

DOI: 10.1039/x0xx00000x

Kimberly A. Scheib, Nathan A. Tavenor, Matthew J. Lawless, Sunil Saxena, W. Seth Horne*

Metal-binding peptides are versatile building blocks in supramolecular chemistry. We recently reported a class of crystalline materials formed through a combination of coiled-coil peptide self-association and metal coordination. Here, we probe the serendipitously discovered metal binding motif that drives the assembly and apply these insights to exert rational control over structure and morphology in the materials.

Many proteins in nature feature metal binding sites on their surfaces or sequestered in cavities. The metals bound at these sites play diverse roles, facilitating folding, molecular recognition, signaling, and catalysis. Beyond natural systems, harnessing metals in protein contexts is a powerful tool in protein engineering and *de novo* protein design.[1] An important complementary aspect of metals in this regard is their use in constructing protein-based supramolecular assemblies.[2]

Inspired precedent showing the structural and functional potential of lattices formed by reticular synthesis involving multidentate small molecule ligands and metals,[3] chemists have worked to establish analogous approaches in which folded protein domains serve as the metal-binding junctions. Pioneering efforts have shown that introduction of metal binding sites in non-metal binding folds can direct self-assembly to form metalloprotein lattices that are both predictable and highly tunable.[4] More recently, the resulting supramolecular materials have been advanced toward functional ends.[5]

In the construction of metal-directed lattices, synthetic peptides represent an attractive ligand class that combines advantages of small-molecule- and protein-based approaches.[6] Proteins and synthetic peptides share the structural modularity inherent to the polypeptide backbone; however, the accessibility of the latter by total chemical synthesis allows ligand designs to depart significantly from natural constraints of covalent connectivity. Such modification can be leveraged to drive interaction with metals, control folding, as well as bring new functions to a material. Compared to small molecules, synthetic peptide ligands offer an added dimension of structural complexity in the form of sequence-encoded folding. While folds accessible to peptides are limited compared to larger proteins, significant information content with respect to secondary structure and interchain assembly can be specified.

A number of reports have demonstrated the power of joining metals and peptide self-assembly in the construction of supramolecular materials.[7] We recently reported one such system based on coiled-coil forming sequences with 2,2′:6′,2″-terpyridine (Tpy) side chains.[8] These efforts highlighted the promise of combining the modular and tunable coiled-coil platform[9] with this abiotic metal-binding moiety;[10] however, the system fell short in one key regard—predictability. Exerting simultaneous control over sequence-encoded folding and intermolecular association by orthogonal forces poses a significant challenge. Addressing this challenge is important, as it advances the resulting materials beyond curiosities to something that can be rationally engineered.

In our original design, we envisioned that the peptides would associate through coiled-coil oligomerization and interaction between coiled coils through bis-Tpy binding to divalent metals (Fig. 1A). Cu^{2+} was found to be privileged in its ability to yield crystalline materials. Most junctions between coiled coils in these lattices consisted of a coordination of Cu^{2+} by a Tpy on one peptide and a glutamic acid (Glu) carboxylate on another (Fig. 1B). While Cu^{2+} is known to favor such ternary complexes,[11] bis-Tpy coordination is also plausible.[12] Thus, we questioned whether the metal coordination behavior observed in the crystals is representative of the interactions driving the association of folded coiled coils in solution. Further, if the serendipitously discovered role of carboxylate side chains is essential to metal-directed assembly, are Tpy-functionalized coiled coils a useful platform for constructing rationally designed architectures? Herein, we seek to understand and control the interactions that drive supramolecular assembly.

Department of Chemistry, University of Pittsburgh, Pittsburgh, PA 15260, USA. E-mail: horne@pitt.edu

† Electronic Supplementary Information (ESI) available: See DOI: 10.1039/x0xx00000x

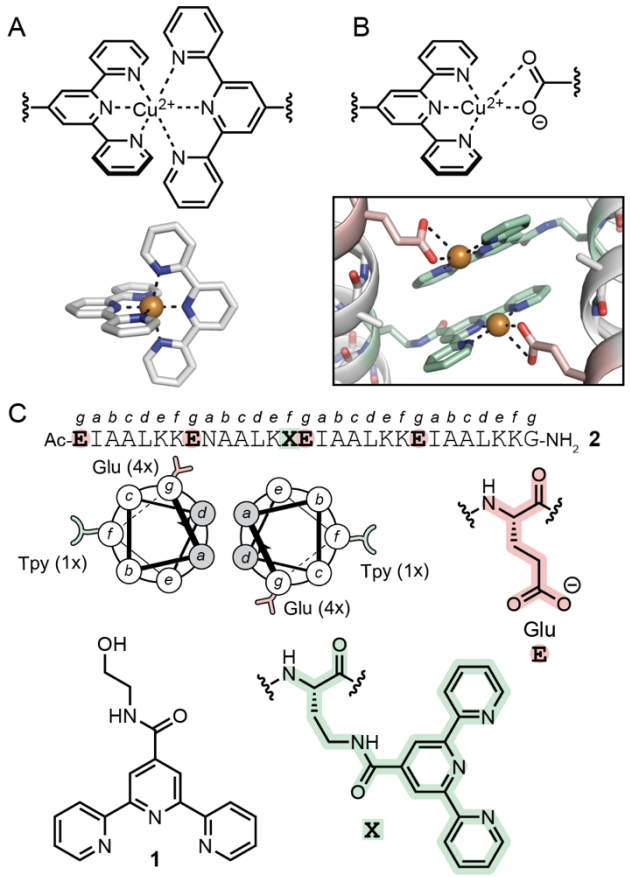

Fig. 1 (A) Coordination of Cu^{2+} by two Tpy ligands and representative crystal structure (CSD 1108163). (B) Coordination of Cu^{2+} by Tpy and carboxylate ligands and representative crystal structure (PDB 5U5B). (C) Structures of ligand **1** and peptide **2**. A helical wheel diagram shows heptad positions of metal-binding residues (highlighted) relative to the hydrophobic core.

Toward the first goal, we synthesized two compounds (see ESI for details): a small molecule (**1**) that is an analogue of Tpy-functionalized unnatural amino acid residue **X** and a peptide (**2**) with a single **X**-residue Tpy moiety. Ligand **1** serves as a control for probing Tpy interaction with Cu^{2+} in dilute aqueous solution absent the peptide context. Peptide **2** (Fig. 1C) is based on a previously reported *de novo* sequence that folds and assembles to form a dimeric coiled-coil quaternary structure.[13] The influence of individual residues on the fold can be best understood by considering their position in the seven-residue, two-turn repeat of the α-helix when part of a coiled-coil.[9] By convention, heptad positions are denoted *a*-*g*, and the hydrophobic interface between helices consists of residues at *a* and *d* positions. Peptide **2** has predominantly isoleucine (Ile) at *a* positions and leucine (Leu) at *d* positions to favor a two-chain assembly.[14] Specificity for the dimeric oligomerization state is further enforced by a single polar *a*-position asparagine (Asn).[15] Peptide **2** has a single **X** residue at a solvent-exposed *f* position midway along the sequence. Thus, the dimeric folded state should project two metal-binding **X**-residue Tpy moieties approximately normal to the coiled-coil axis. Peptide **2** also bears four solvent-exposed Glu residues at *g* heptad positions that could compete with Tpy groups in metal-directed inter-chain assembly.

We performed a panel of electron paramagnetic resonance (EPR) spectroscopy experiments to compare the interactions of **1** and **2** with Cu^{2+} under dilute aqueous conditions (300 μM Tpy). In the 80 K continuous wave (CW) EPR spectra obtained upon titration of **1** with Cu^{2+} (Fig. 2A), the hyperfine and g-tensor parameters at a range of 0.3-1 equiv. metal are consistent with three equatorial nitrogens (from Tpy) and one equatorial oxygen (attributed to water).[16] The hyperfine parameters and spectral features for the bis-Tpy coordination mode were not observed at any ratio of metal to **1**.[17]

Circular dichroism (CD) scans and thermal melts of peptide **2**, indicated a stable coiled-coil fold (Fig. S1). In order to trap and characterize early intermediates formed in the metal-mediated self-assembly process, samples were flash frozen after addition of Cu^{2+} prior to EPR measurements. CW data for **2** (Fig. 2A) show a similar metal coordination environment as seen for **1**, although the superhyperfine structure was not resolved. In the case of peptide **2**, the equatorial oxygen could originate from either water, a Glu side chain, or some other functional group.

We performed 2D hyperfine sublevel correlation (HYSCORE) EPR to probe atoms distal to the Cu^{2+} centers in each sample.[18] The HYSCORE spectra for samples of **1** and **2** in the presence of 0.5 equiv. Cu^{2+} (Fig. 2B) show strong cross-peaks from distal hydrogens (~14 MHz).[19] Peptide **2**, but not ligand **1**, has additional peaks for distal nitrogen atoms (~2-4 MHz).[20] This feature is consistent with Tpy-Tpy π-stacking, a motif commonly observed at the metal-mediated junctions between chains in

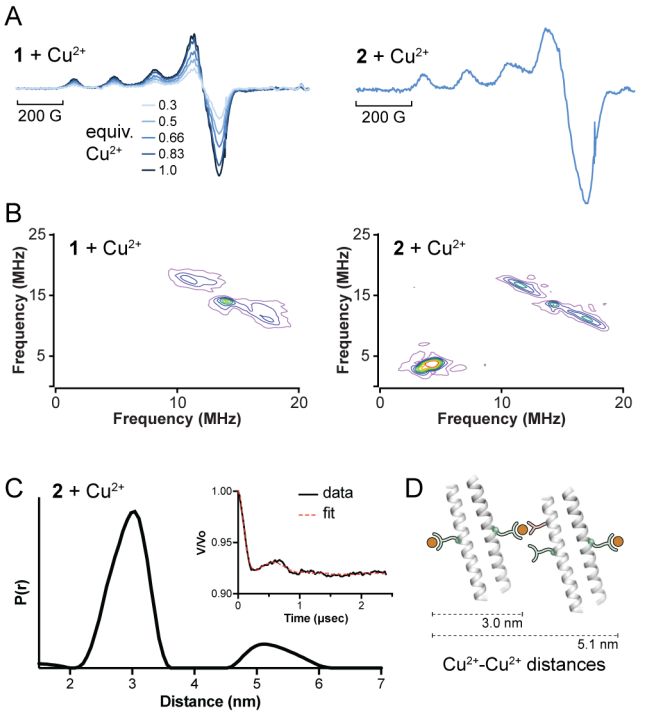

Fig. 2 (A) CW EPR spectra of ligand **1** and peptide **2** in the presence of Cu^{2+} (0.3-1.0 equiv. for **1**, 0.5 equiv. for **2**). (B) HYSCORE spectra of ligand **1** and peptide **2** in the presence of 0.5 equiv. Cu^{2+}. (C) DEER distance distribution observed for peptide **2** in the presence of 0.5 equiv. Cu^{2+}; inset shows the baseline corrected DEER signal and fit. (D) Simplified cartoon accounting for the two Cu-Cu distances observed by DEER. All samples are 300 μM ligand in 40 mM NEM, pH 7.4.

prior crystal structures (Fig. 1B).[8] The absence of distal nitrogen signal for ligand **1** suggests that hydrophobic interactions alone are insufficient to drive the association of Tpy moieties under the dilute conditions of the experiment. Thus, HYSCORE results for **2** support the hypothesis that at least a subset of the equatorial oxygen ligands on Tpy-bound Cu^{2+} observed by CW are from a Glu residue on a neighboring peptide chain. It is this Glu coordination that brings the second coiled coil and its Tpy side chain in proximity to the first (Fig. 2D).

The above EPR data suggest Tpy-Cu^{2+}-Glu coordination is the preferred assembly mode for the Tpy-functionalized peptides. Cu^{2+} based Double Electron-Electron Resonance (DEER)[21] spectroscopy measurements on peptide **2** were carried out to further corroborate this model by measuring distances between pairs of Cu^{2+} centers in the assemblies.[22] The distance distribution for **2** (Fig. 2C) shows two predominant metal-metal distances at 3.0 nm and 5.1 nm. The former is consistent with the distance between Cu^{2+} ions across a single coiled coil, while the latter is evidence of Cu^{2+} centers separated by two coiled-coil units (Fig. 2D).[23] Support for the interpretation of the DEER results comes from the observation of an increase in distance between Cu^{2+} centers when peptide **2** is replaced in the experiment by an analogue in which the **X**-residue side chain is extended by two methylene units (Fig. S2).

Having gained new insights into the metal-directed assembly of the Tpy-functionalized peptides, we sought to apply this knowledge to exert rational control over assembly morphology. Our initial report included one sequence that was designed to form hexagonal supramolecular lattice made up of trimeric coiled-coil junctions.[8] While the peptide adopted the expected trimeric fold, it failed to form the anticipated lattice due to the non-specific participation of Glu side chains in the assembly. In an effort test the viability of refined design principles based on a superior understanding of the forces driving assembly, we designed two new peptides with the goal of producing the unobtained hexagonal net.

Based on a previously reported *de novo* designed trimeric coiled coil,[13] peptides **3** and **4** (Fig. 3) contain Ile residues at *a* and *d* heptad positions to specify stoichiometry.[14] Glu residues in the original sequence were replaced by either Gln or Ala to maintain solubility while not significantly destabilizing the fold. A single Tpy residue was placed in each sequence at a solvent-exposed *f* position, and a Glu residue was incorporated at an *f* position two heptads away. Peptides **3** and **4** differ only in the relative placement of their two metal-binding moieties, which was intended in both cases to direct the formation of a hexagonal lattice with vertices made up of trimeric coiled coils and struts composed of Cu^{2+} bound by Tpy and Glu moieties on neighboring chains.

CD scans of peptides **3** and **4** showed spectral features consistent with a well-folded coiled coil (Fig. S1). Thermal melts showed cooperative unfolding transitions with midpoints that were high (66 °C for **3** and 77 °C for **4**), albeit somewhat lower than the prototype trimer that inspired their design (> 90 °C).[13] This decrease in stability is attributed to loss of interchain salt bridges from mutation of Glu residues and helix-disruption from the bulky **X**-residue side chain. Small differences in stability notwithstanding, the CD results indicate that **3** and **4** are well-folded under dilute aqueous conditions.

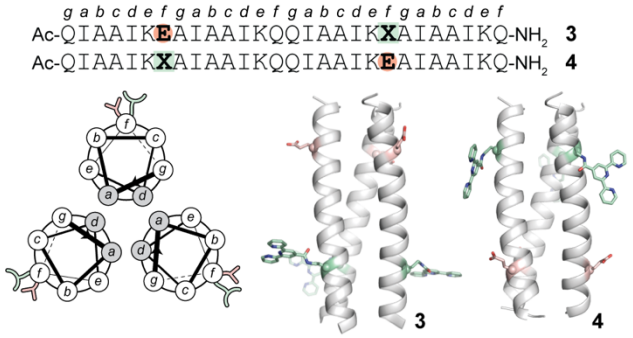

Fig. 3 Sequences, helical wheel diagram, and crystal structures of trimeric coiled-coil peptides **3** (PDB 6OLN) and **4** (PDB 6OLO). Metal-binding residues are shown as sticks, with color scheme matching Fig. 1.

In order to probe the lattices resulting from metal-directed assembly of **3** and **4**, we crystallized each in the presence of Cu^{2+} by hanging drop vapor diffusion and determined the structures by X-ray crystallography. Crystals of **3** were grown from a buffer consisting of 0.1 M Bis-Tris pH 6.5, 25% w/v PEG 3350, and 5 mM $CuCl_2$. The structure was solved to 2.5 Å resolution and refined to an R/R_{free} 0.27/0.30. Crystals of peptide **4** were grown from a buffer composed of 0.1 M Tris pH 8.5, 25% w/v PEG 3350, 5 mM $CuCl_2$. The structure was solved to 2.3 Å resolution and refined to an R/R_{free} of 0.26/0.27.

As intended, **3** and **4** both adopt parallel trimeric coiled-coil folds with solvent-exposed metal-binding residues about the periphery (Fig. 3). In the case of **3**, the asymmetric unit contains six chains arranged in two crystallographically distinct but highly similar trimers (0.44 Å C_α rmsd). For peptide **4**, the asymmetric unit consists of a single chain and the trimeric coiled coil sits on a crystallographic 3-fold symmetry axis. The quaternary structures for **3** and **4** show high homology to each other (0.60 Å C_α rmsd) as well as to the sequence that inspired their design (PDB 4DZL; 0.51 Å C_α rmsd for overlay of **3**, 0.72 Å C_α rmsd for overlay of **4**) (Fig. S3).[13]

Turning to the details of the metal-directed supramolecular assemblies, peptide **3** realized some but not all aspects of our design for its intended behavior. All the contacts between neighboring coiled coils in the lattice are mediated by **X** and/or Glu residues. Out of six Tpy moieties in the asymmetric unit, three engage in the expected Tpy-Cu^{2+}-Glu coordination (Fig.

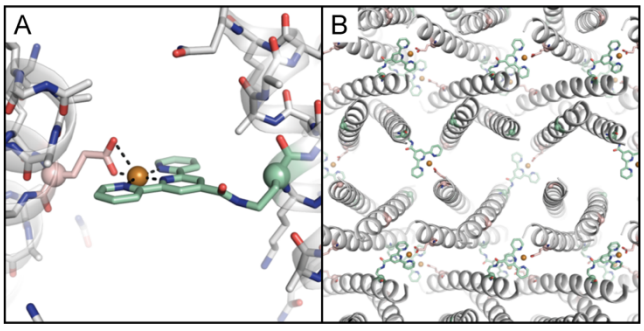

Fig. 4 Views of crystal structure of peptide **3** (PDB 6OLN). (A) Representative Tpy-Cu-Glu coordination motif. (B) Cu-mediated contacts in a single layer (*ab* plane) of the lattice.

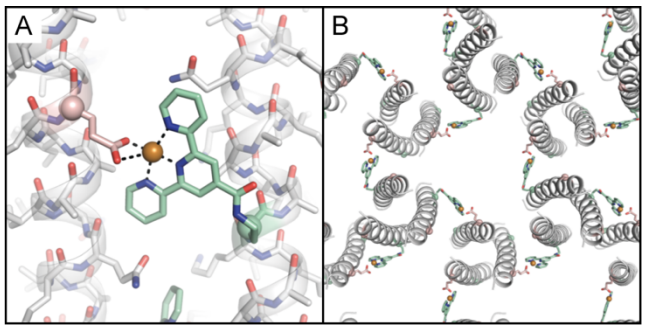

Fig. 5 Views of crystal structure of peptide **5** (PDB 6OLO). (A) Representative Tpy-Cu-Glu coordination motif. (B) Cu-mediated contacts in a single layer (*ab* plane) of the lattice.

4A). Three others are bound to Cu^{2+} but not to a Glu residue and instead engage in π-stacking interactions with **X** residues from neighboring chains (Fig. S4). Because of these differences in coordination behavior among the Tpy moieties, the lattice did not manifest the intended hexagonal net morphology (Fig. 4B).

A noteworthy feature of the crystal obtained for peptide **4** with Cu^{2+} (Fig. 5) was the high symmetry of the lattice. The single **X** residue Tpy moiety in the asymmetric unit, and thus every Tpy in the crystal, engages in the expected Tpy-Cu^{2+}-Glu coordination between chains. The result is a hexagonal network of trimeric coiled coils held together entirely through metal coordination from neighboring chains. The only aspect of the assembly formed by **4** that differed from our design is the relative orientation of adjacent trimers in the lattice; we had intended an antiparallel arrangement but observed a parallel relative orientation instead (Fig. S5).

In summary, we have shown that a serendipitously discovered metal-directed assembly mode of peptides bearing carboxylate and Tpy side chains can be leveraged for the rational construction of a defined supramolecular lattice. These results underscore the power of EPR for probing complex macromolecular assemblies and lay the groundwork for the design of new architectures, including crystalline materials and soluble assemblies, through the systematic placement of metal-binding residues in coiled-coil scaffolds.

Conflicts of interest

There are no conflicts to declare.

Notes and references

‡ Funding for this work was provided, in part, by the National Science Foundation (DMR1149067 to W.S.H. and MCB1613007 to S.S.). Additional support for instrumentation was provided by the National Science Foundation (MRI 1625002 and 1725678).

1 (a) Y. Lu, N. Yeung, N. Sieracki and N. M. Marshall, *Nature*, 2009, **460**, 855; (b) A. F. A. Peacock, *Curr. Opin. Chem. Biol.*, 2013, **17**, 934-939; (c) F. Yu, V. M. Cangelosi, M. L. Zastrow, M. Tegoni, J. S. Plegaria, A. G. Tebo, C. S. Mocny, L. Ruckthong, H. Qayyum and V. L. Pecoraro, *Chem. Rev.*, 2014, **114**, 3495-3578; (d) O. F. Brandenberg, R. Fasan and F. H. Arnold, *Curr. Opin. Biotechnol.*, 2017, **47**, 102-111; (e) U. Markel, D. F. Sauer, J. Schiffels, J. Okuda and U. Schwaneberg, *Angew. Chem. Int. Ed.*, 2019, **58**, 4454-4464.

2 E. N. Salgado, R. J. Radford and F. A. Tezcan, *Acc. Chem. Res.*, 2010, **43**, 661-672.

3 (a) M. Kondo, T. Yoshitomi, H. Matsuzaka, S. Kitagawa and K. Seki, *Angew. Chem. Int. Ed.*, 1997, **36**, 1725-1727; (b) H. Li, M. Eddaoudi, T. L. Groy and O. M. Yaghi, *J. Am. Chem. Soc.*, 1998, **120**, 8571-8572; (c) J. S. Seo, D. Whang, H. Lee, S. I. Jun, J. Oh, Y. J. Jeon and K. Kim, *Nature*, 2000, **404**, 982-986; (d) N. L. Rosi, J. Eckert, M. Eddaoudi, D. T. Vodak, J. Kim, M. O'Keeffe and O. M. Yaghi, *Science*, 2003, **300**, 1127-1129; (e) L. Ma, J. M. Falkowski, C. Abney and W. Lin, *Nat. Chem.*, 2010, **2**, 838-846; (f) E. D. Bloch, W. L. Queen, R. Krishna, J. M. Zadrozny, C. M. Brown and J. R. Long, *Science*, 2012, **335**, 1606-1610.

4 (a) Y. Suzuki, G. Cardone, D. Restrepo, P. D. Zavattieri, T. S. Baker and F. A. Tezcan, *Nature*, 2016, **533**, 369; (b) J. B. Bailey, L. Zhang, J. A. Chiong, S. Ahn and F. A. Tezcan, *J. Am. Chem. Soc.*, 2017, **139**, 8160-8166.

5 W. J. Song and F. A. Tezcan, *Science*, 2014, **346**, 1525-1528.

6 R. Zou, Q. Wang, J. Wu, J. Wu, C. Schmuck and H. Tian, *Chem. Soc. Rev.*, 2015, **44**, 5200-5219.

7 (a) G. W. M. Vandermeulen, C. Tziatzios, D. Schubert, P. R. Andres, A. Alexeev, U. S. Schubert and H.-A. Klok, *Aust. J. Chem.*, 2004, **57**, 33-39; (b) D. E. Przybyla and J. Chmielewski, *J. Am. Chem. Soc.*, 2008, **130**, 12610-12611; (c) S. N. Dublin and V. P. Conticello, *J. Am. Chem. Soc.*, 2008, **130**, 49-51; (d) S. Tangbunsuk, G. R. Whittell, M. G. Ryadnov, G. W. M. Vandermeulen, D. N. Woolfson and I. Manners, *Chem. Eur. J.*, 2012, **18**, 2524-2535; (e) M. Nepal, M. J. Sheedlo, C. Das and J. Chmielewski, *J. Am. Chem. Soc.*, 2016, **138**, 11051-11057; (f) T. Ghosh, N. Fridman, M. Kosa and G. Maayan, *Angew. Chem. Int. Ed.*, 2018, **57**, 7703-7708; (g) R. Misra, A. Saseendran, S. Dey and H. N. Gopi, *Angew. Chem. Int. Ed.*, 2019, **58**, 2251-2255.

8 N. A. Tavenor, M. J. Murnin and W. S. Horne, *J. Am. Chem. Soc.*, 2017, **139**, 2212-2215.

9 D. A. Parry, R. D. Fraser and J. M. Squire, *J. Struc. Biol.*, 2008, **163**, 258-269.

10 E. C. Constable, *Chem. Soc. Rev.*, 2007, **36**, 246-253.

11 H. Sigel, *Angew. Chem. Int. Ed.*, 1975, **14**, 394-402.

12 R. Calì, E. Rizzarelli, S. Sammartano and G. Siracusa, *Transition Met. Chem.*, 1979, **4**, 328-332.

13 J. M. Fletcher, A. L. Boyle, M. Bruning, G. J. Bartlett, T. L. Vincent, N. R. Zaccai, C. T. Armstrong, E. H. C. Bromley, P. J. Booth, R. L. Brady, A. R. Thomson and D. N. Woolfson, *ACS Synth. Biol.*, 2012, **1**, 240-250.

14 (a) P. Harbury, T. Zhang, P. Kim and T. Alber, *Science*, 1993, **262**, 1401-1407; (b) D. N. Woolfson and T. Alber, *Protein Sci.*, 1995, **4**, 1596-1607.

15 X. Zeng, A. M. Herndon and J. C. Hu, *Proc. Natl. Acad. Sci. USA*, 1997, **94**, 3673-3678.

16 J. Peisach and W. E. Blumberg, *Arch. Biochem. Biophys.*, 1974, **165**, 691-708.

17 R. Bonomo and F. Riggi, *Transition Met. Chem.*, 1984, **9**, 308-311.

18 P. Höfer, A. Grupp, H. Nebenführ and M. Mehring, *Chem. Phys. Lett.*, 1986, **132**, 279-282.

19 S. A. Dikanov, R. I. Samoilova, D. R. J. Kolling, J. T. Holland and A. R. Crofts, *J. Biol. Chem.*, 2004, **279**, 15814-15823.

20 (a) S. A. Dikanov, L. Xun, A. B. Karpiel, A. M. Tyryshkin and M. K. Bowman, *J. Am. Chem. Soc.*, 1996, **118**, 8408-8416; (b) K. I. Silva, B. C. Michael, S. J. Geib and S. Saxena, *The Journal of Physical Chemistry B*, 2014, **118**, 8935-8944.

21 M. Pannier, S. Veit, A. Godt, G. Jeschke and H. W. Spiess, *J. Magn. Reson.*, 2000, **142**, 331-340.

22 M. Ji, S. Ruthstein and S. Saxena, *Acc. Chem. Res.*, 2014, **47**, 688-695.

23 N. A. Tavenor, K. I. Silva, S. Saxena and W. S. Horne, *J. Phys. Chem. B*, 2014, **118**, 9881-9889.

TOC Figure and text for Scheib, et al.

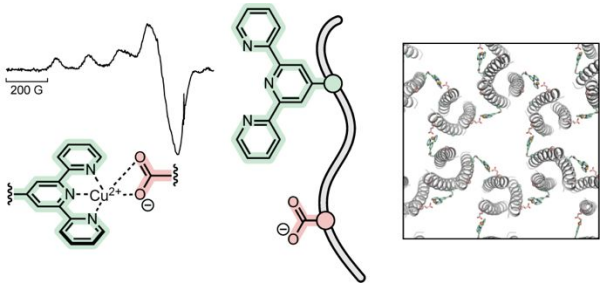

Spectroscopic elucidation of the interaction between terpyridine-functionalized coiled-coil peptides and Cu(II) enables the construction of rationally designed supramolecular lattices.